Structure of nitrogenated carbon films by electron diffraction and imaging

Somnath Bhattacharyya,* O. Madel, S. Schulze, P. Häussler, M. Hietschold, and F. Richter
Institut für Physik, TU–Chemnitz, D-09107 Chemnitz, Germany
(Received 3 May 1999)

The change of the microstructure of carbon films after nitrogen incorporation is a topic of extensive discussion. Concerning this topic, tetrahedral amorphous carbon prepared by filtered cathodic arc deposition is chosen for present investigations where nitrogen is incorporated in the films by using a Kaufman-type ion source. The average distribution of bonds and bond angles is studied by electron diffraction leading to the radial distribution function. On the other hand, a detailed study on the film microstructure has been carried out in a high-resolution transmission electron microscope. Nanocrystalline structures of nitrogenated carbon are clearly seen, especially, from the films having high nitrogen concentration. The variation of structure of the films with nitrogen concentration is understood from electron energy loss spectra. The bonding arrangement of carbon and nitrogen atoms is thoroughly emphasized from carbon as well as nitrogen *K* edges. The microscopic view helps us to understand a model of carbon and carbon-nitrogen nanostructures.

I. INTRODUCTION

The nitrogen doping of amorphous carbon and tetrahedral amorphous carbon (ta-C) films is to some extent a subject of controversy.[1–6] One of the main reasons for that is the limited knowledge on film microstructure and its influence on electronic structure.[2] Researchers have tried to establish from electron diffraction, radial distribution function (RDF), and electron energy loss spectroscopy (EELS) that there is a strong indication of change of electronic structure as well as doping of the diamondlike carbon.[5–8] RDF can only determine average local structures,[9–11] whereas the microstructure can be understood from microscopy, e.g., high-resolution transmission electron microscope (HRTEM) imaging. Accordingly, the understanding of the structure of CN_x films at nanometer scale is hardly possible from RDF due to the complexity of different CN bonding arrangements. Up to now there are no reports on crystalline β-C_3N_4 of micron size.[7,8] All crystallites are likely to be confined in the nanometer range. Other crystalline phases of CN_x are suggested as well, for instance α-C_3N_4, cubic C_3N_4, and rhombohedral C_3N_4 type.[11] Reports are found on zinc blende or fullerene or onion-type structures of nitrogenated carbon.[7] So we emphasize the importance of a detailed study of our samples by electron diffraction and imaging (by HRTEM). A small percentage of nitrogen can produce sp^2-bonded structures.[3] It is difficult to separate the contribution of C-C and different CN bonds including single, double, and triple bonds.[1] So the structure of CN_x films is obviously not a random mixture of different hybridization bonds. Besides, there is a need for understanding the electronic properties and the density of states corresponding to the nanostructure region. EELS is sensitive to the local coordination of CN structure, which can be useful to distinguish carbon nanostructures. These experiments are useful at carbon *K* edge (C *K* edge) for carbon nanostructures and also at the nitrogen *K* edge (N *K* edge) edge for understanding the environment of nitrogen atoms. Particularly, the N *K* edge has not been well studied before, which disables us to understand CN and NN bonds. In addition, a systematic study is lacking on the change of CN_x local structures as a function of nitrogen content.

In a conventional filtered cathodic arc technique (evaporation of graphite) where nitrogen is introduced from the gas phase, the formation of crystalline phases of CN_x, particularly crystalline β-C_3N_4, seems to be unlikely because nitrogen has to substitute the carbon atoms from the planar sp^2-bonded configuration. Using a Kaufman-ion source a highly dense energetic nitrogen-ion flux can be obtained, which is helpful to incorporate a high nitrogen concentration into ta-C films. With this technique, therefore, we have the possibility to modify short-range order in CN_x films.

The second important motivation of this work is to reinvestigate the role of sp^2 bonding in nitrogen-free ta-C films. Theoretically[9] as well as by electron diffraction experiments[5] it was revealed that a compressed graphitic layered structure was needed to get an agreement between calculations and experimental results. It is very important to have a clear understanding on the sp^2-bonded local structure, which could be responsible for discarding the utility of this material as a good electronic material.

The paper is arranged as follows. Having explained the experimental and structural properties of this material in Sec. II, the average structure from RDF is presented (Secs. III A and III B). In the following part of this section (Sec. III C) the microstructure of different CN_x films will be focused. The importance of these microstructures will be explained by EELS (Sec. III D).

II. EXPERIMENTAL DETAILS

A combination of a filtered cathodic arc with a Kaufman-type ion source is used for the sample preparation, where energy and flux of carbon and nitrogen ions can be controlled independently. A graphite disc of high purity (Carbon SGL Co) and density of 1.9 g/cm^3 is used for the cathode. A stream of carbon plasma (mean ion energy of about 26 eV with respect to ground and ~36 eV with respect to cathode) is passed through a magnetic coil that filters neutral carbon atoms and macroparticles. Nitrogen is introduced in the films

TABLE I. Description of the samples properties obtained from ERDA, TEM, and EELS. The subscript x of a-CN_x denotes the atomic concentration of nitrogen only.

Samples	N at. % (± 1)	sp^2 fraction	Density (g/cm^3)	Microstructure (with amorphous regions)
ta-C	00	0.3	2.98	Ordered graphic showing diffraction rings
a-CN_{04}	04			
a-CN_{09}	09	0.4	2.94	Sharp rings in diffraction
a-CN_{12}	12			Weak crystalline peak and diffraction rings
a-CN_{15}	15			
a-CN_{19}	19	0.46	2.89	Low intense crystalline
a-CN_{25}	25			Feature of α-C_3N_4 and diffraction rings
a-CN_{29}	29	1.23	2.27	Sharp peaks similar to β-C_3N_4, No halo nor ordered graphite.

by the admittance of a gas flow or by the bombardment of the growing film with nitrogen ions from the Kaufman-ion source. With a flow rate of 3 SCCM (cubic centimeter per minute at STP) the gas pressure in the chamber is maintained at about 2×10^{-2} Pa. The films are deposited on silicon (100) substrates, which are cleaned by ethanol and argon ion beam before deposition. The substrates are mounted on a water-cooled copper plate. No substrate bias was applied. The stoichiometry and density of all the films are determined by elastic recoil-detection analysis (ERDA).

The samples of about 40 nm thickness are prepared on small copper grids for electron microscopy by dissolving the silicon substrates in HF/HNO_3 acid and then rinsing into distilled water. Electron diffraction and imaging is performed in a Philips CM20 FEG transmission-electron microscope with a primary electron energy of 200 keV. The electron energy-loss spectra were recorded on a Gatan 666 PEELS spectrometer mounted on the same microscope. The point and line resolution of the microscope are 2.4 Å and 1.4 Å, respectively, and energy resolution of the spectrometer is about 1 eV. The spectral data are analyzed by Gatan EL/P software (version 2.1) to calculate the thickness of the samples to remove multiple scattering. The plasmon energy is calculated from the peak maximum $E_{\max}$ and from the full width at half maximum ΔEp as $Ep=(E_{\max}^2+\Delta E_p^2/4)^{1/2}$. Following Berger *et al.*[11] the fraction of sp^2 bonds is calculated from $R=(I_\pi/I_{CN})[I_\pi(e)/I_{CN}(e)]$, where I_{CN} and $I_{CN}(e)$ are the total intensities in both the π^* and σ^* peaks (integrated over an energy of $\sim$50 eV) for the CN_x films and for electron beam evaporated carbon, respectively. Intensities of π^* peaks only are denoted by I_π and $I_\pi(e)$, for CN_x and the evaporated carbon, respectively. Multiple scattering contributions are removed by Fourier-Ratio method, i.e., dividing the Fourier transform of K-shell spectrum by the corresponding Fourier transform of low-loss spectrum, followed by an inverse Fourier transformation.

For the calculation of the RDF the intensity of diffracted electrons is converted to the pair correlation function $G(r)=8\pi\int_0^{K_{\max}}KI(K)\sin Kr\,dK$, with $K=2\sin\theta/\lambda$ and $I(K)=[I'(K)Nf^2]K/Nf^2$ the interference function. $I'(K)$ and Nf^2 are energy filtered scattering intensity and the scaled atomic-scattering intensity, respectively. λ is the wavelength of scattered electrons. The radial distribution function $J(r)$ is calculated from $G(r)$, $J(r)=4\pi r^2\rho+rG(r)$ (where ρ corresponds to the average number density of atoms in the samples), which is a measure of the number of electrons at a given distance r. A series of Gaussians are used to fit $J(r)$.

III. RESULTS AND DISCUSSION

The atomic percentage of nitrogen, the sp^2-fraction and the density of a complete batch of samples are given in Table I. Average distributions of bonds using pair correlation function $G(r)$ and $J(r)$ are performed on three of the samples having 0%, 19%, and 29% of nitrogen and the results are summarized in Table II. The $G(r)$ and $I(K)$ of these samples are shown in the Figs. 1(a) and 1(b). Decomposition of the $J(r)$ is presented in Figs. 2(a)–2(c). The average bond angle (θ) is calculated from $\theta=2\sin^{-1}(r_2/2r_1)$, where r_1 and r_2 represent the first- and the second-nearest-neighbor distances. The atomic number densities of the samples are calculated from the slopes of $G(r)$ at low r values [see Fig. 1(a)].

A. Pair correlation function [$G(r)$]

The position of the first- and the second-nearest-neighbors decreases from ta-C to a-CN_{29}. The average bond angle rises from 112.0° to 120.0° in these samples. The atomic number density (ρ) of the samples is found to decrease with nitrogen

TABLE II. Variation of nearest-neighbor distances, bond angle, coordination number, and atomic number density calculated from $G(r)$ and $J(r)$. A_1 and A_2 are the areas under first and second intense peak in $J(r)$.

	Nitrogen at. %	r_1 (Å)	r_2 (Å)	r_{12} (Å)	A_2/A_1	Bond angle	Coordin. number	At. density (ρ) (Å^{-3})
ta-C	0.0	1.52	2.52	2.02	2.55	112.0°	3.60	0.164
a-CN_{09}	9.0	1.47	2.43	1.98	2.50	112.2°	2.90	0.153
a-CN_{29}	29	1.38	2.39	1.86	2.46	120.0°	2.02	0.140

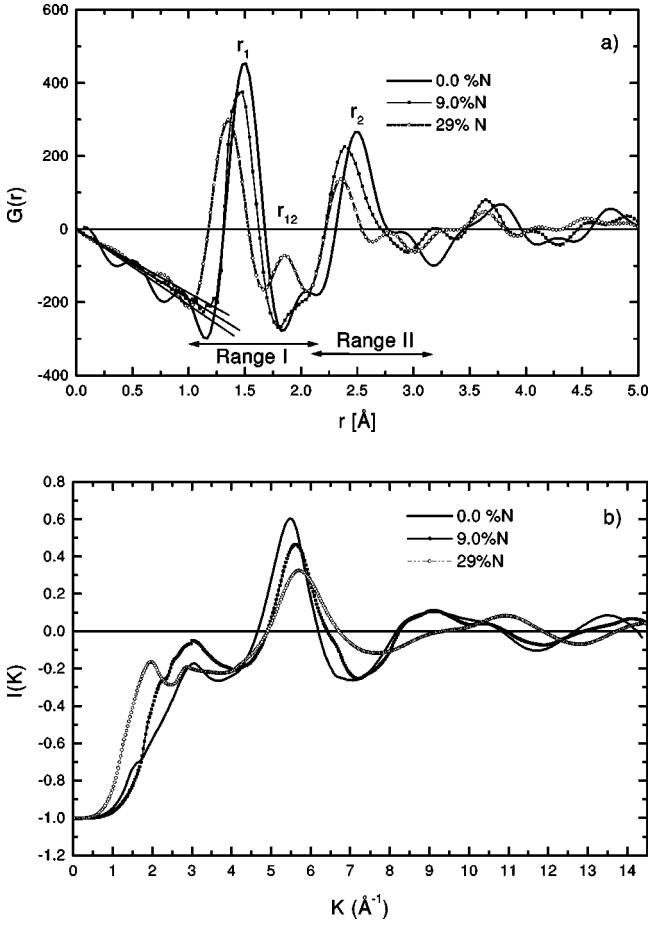

FIG. 1. (a) pair correlation function and (b) interference function derived from electron diffraction of ta-C and nitrogenated carbon films.

concentration (see Table II). The average coordination number of these samples changes from 3.60 (ta-C) to 2.90 (a-CN_{09}) and to 2.02 (a-CN_{29}). These features generally represent that ta-C is diamondlike and a-CN_x films are becoming graphitic with increase of nitrogen concentration. We now discuss with the increase of r, details of $G(r)$ from three different samples selecting a few partially overlapping r ranges [see Fig. 1(a)].

Range I: The first peak position of ta-C at 1.52 Å is very close to the CC bond length of diamond (1.544 Å), which changes to 1.38 Å in a-CN_{29} indicating more trigonal bonded carbon similar to olefinic structure.[5] A small increase of the full width at half maximum (FWHM) of the first peak of a-CN_{29} compared to the ta-C towards the lower r-side may appear due to CC triple bonds (1.203 Å) or CN double and CN triple bonds (1.30 Å and 1.14 Å, respectively). Also there is a possibility of increase of static disorder of the bond length in the CN_x films causing the increase of FWHM.

Previously no good explanation was provided on the region between 1.6 Å and 2.2 Å. A small peak at 2 Å may account for a fourfold bonded network as proposed by Li and Lannin.[10] In fact in the nitrogen-free sample a small peak appears at $r_{12}=2.02$ Å [Fig. 2(a)], in agreement to that. In the nitrogen-doped films a mixed feature is evident in this region. For a-CN_{09} this peak (r_{12}) reduces to a minimum intensity [Fig. 2(b)] and reemerges as an intense peak at 1.86 Å for maximum nitrogen concentration [Fig. 2(c)]. The shift of this peak may be explained by the graphitization. In the previous work by Davis *et al.*[11] a similar small peak is observed, which on the other hand, is shifted towards high r values with nitrogenation. A similar behavior in this region of $G(r)$ is also known for the hypothetical crystalline structures of β-C_3N_4, for cubic C_3N_4 and graphitic CN, but not in the hypothetical rhombohedral C_3N_4 structure.[7,8,11]

Range II: In the case of range II (in between 2.1 and 3.2 Å, where the maximum corresponds to the second-nearest neighborhood), the features are not very straightforward. For example, the assignment of the third-nearest-neighbor peak is not unique. Recalling the structure of diamond and graphite many authors suggested that for ta-C this peak appears at about 3 Å.[5] From molecular dynamics Jungnickel *et al.*[9] suggested (counting the third neighbor along the covalent bonds) that this peak originates from the dihedral torsion of the third neighbored sp^2 and sp^3 units and the peak maximum corresponding to the third-nearest neighbor should be located at about 3.7 Å. Although the a-CN_{29} films are graphitic, the double peak between 2.2 Å and 2.76 Å is similar to that which is seen in crystalline diamond as well as in polycrystalline graphite.[5] However, for this composition the peak at 2.76 Å is also a signature of sp^2-bonded carbon or a hexagonal ring structure. From reverse Monte Carlo simulation of glassy carbon O'Malley *et al.*[9] showed that this peak arises from the significant distortion of hexagonal rings forming a graphitic network. The position at 2.76 Å is exactly the double of the first peak position (1.38 Å). This is a clear evidence of graphitization with hexagonal ring structure.[10] In a-CN_{09} a similar feature is not found due to a small amount of hexagonal rings. In ta-C the peak at 2.9 Å is less than double of the first peak position.

The radial distribution function $J(r)$ is decomposed in the region between 1.0 Å and 2.6 Å into several Gaussians peaks [Figs. 2(a)–2(c)]. The integrated area ratio of second and the first peaks (A_2/A_1) is useful for determining the sp^2 content. These values are 2 and 3 for crystalline graphite and diamond, respectively. For ta-C samples A_2/A_1 is nearer to that of diamond suggesting an sp^3-rich system. The measured values of the ratio of the a-CN_x samples are decreasing with increasing nitrogen content. Although these values are interfered by CN bonds the decrease of these values indicates a transition from sp^3-rich to sp^2-rich systems with the increase of nitrogen concentration.

In the following we compare several peaks obtained from the decomposed redial distribution function of different samples as shown in the Figs. 2(a)–2(c). The width and area of the first peak in the nitrogen-free sample are 0.26 Å and 38.5 Å^2, respectively, which change to 0.27 Å and 25.1 Å^2 due to the presence of 29% nitrogen [Figs. 2(a) and 2(c)]. Although the width for the film with 9% nitrogen is smaller (0.22 Å) than for the other compositions, the peak area comes in between, i.e., 34.5 Å^2. In particular for a-CN_{29} it is difficult to separate the contribution of CN single bonds from RDF curve as the bond length is in between 1.35 and 1.39 Å. Other peaks corresponding to CN bonds may be covered under the intense peak of CC bonds. For example, the first intense peak of a-CN_{09} is asymmetric towards the low r region where a contribution from C≡N($\sim$1.14 Å), C═N ($\sim$1.30 Å), C≡C($\sim$1.18 Å) or from N═N($\sim$1.24 Å) can be expected. Neglecting the presence of CN bonds at short

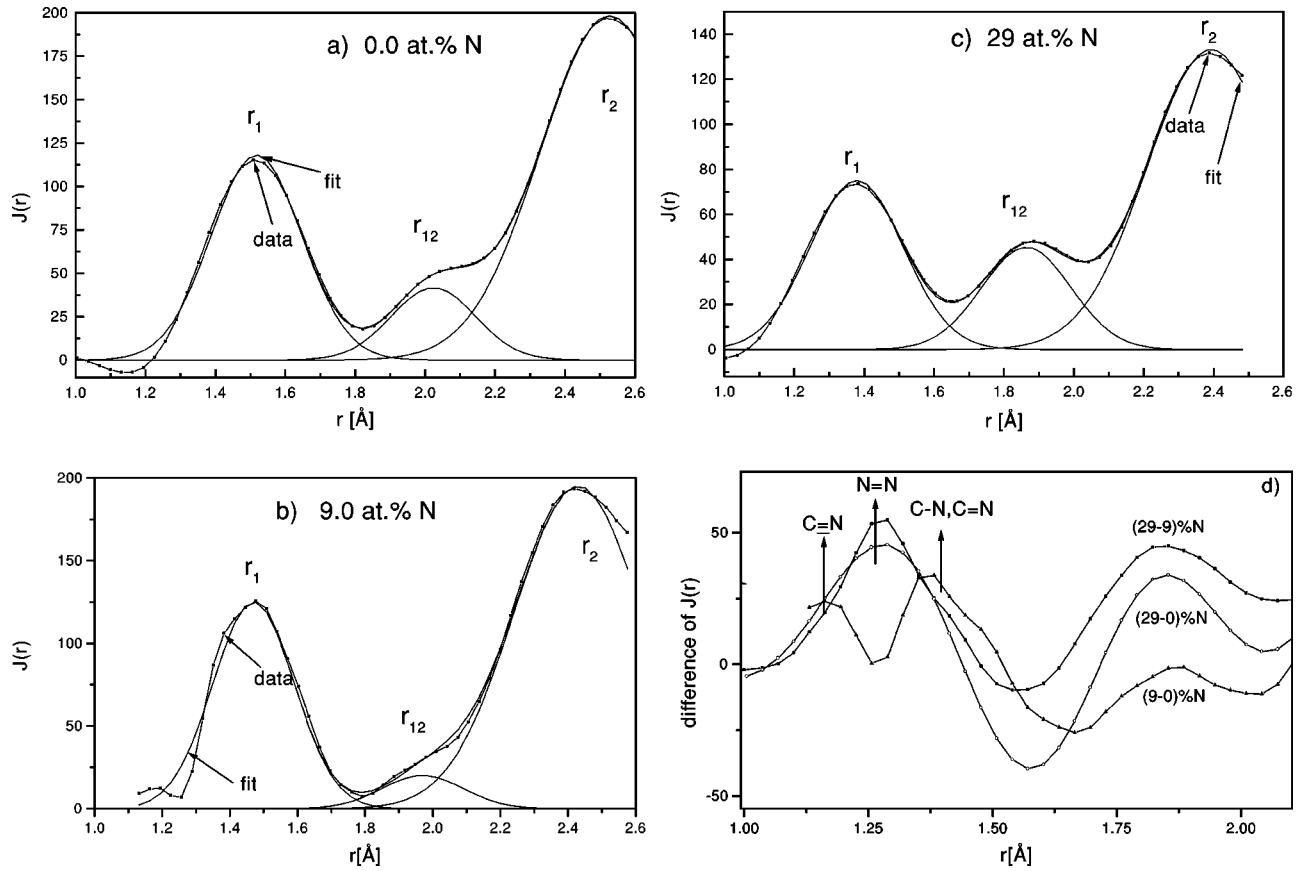

FIG. 2. Decomposed RDF indicating a distribution of bonds lengths of atoms of carbon films having (a) 0%, (b) 19%, and (c) 29% nitrogen, respectively. (d) Difference curve of $J(r)$ with respect to nitrogen concentration.

range this decrease is correlated with the reduction of mass density of the samples. The position, width and area of the small intermediate peak between the first- and the second-nearest neighborhood (r_{12} in Table II) change from 2.02 Å, 0.240 Å, and 12.57 Å^2 in the nitrogen-free samples to 1.86 Å, 0.255 Å, and 14.51 Å^2, respectively, for 29% nitrogen incorporation. This difference may be possible if we allow a second bonding configuration, e.g., CN bonds. In general, the origin of this part is not established. It might also happen due to a bond disorder and dangling bonds in the carbon matrix.

Shift of position of the nearest neighbors and variation of mass density of amorphous carbon have been correlated by Wang *et al.*[9] A similar feature is holding good for the present nitrogenated carbon, where with the decrease of the mass density the second nearest neighbor shifts towards a lower r (from 2.52 Å to 2.43 Å) value. The decrease in area of the first peak in $J(r)$ corresponds to a decrease of sp^3 content. But the area of the second peak is described by $N_c(N_c-1)$, where N_c stands for the coordination number of the material. So a decrease of the sp^3 content results in the decrease of the area under the second neighbor much more than in that of the number of first neighbors. The area under this peak also decreases from 98.4 Å^2 in ta-C to 61.7 Å^2 in a-CN_{29} suggesting a decrease of sp^3 fraction in the films upon nitrogen incorporation. The width of this peak is higher than the first peak, this reflects a contribution due to the presence of a static variation in the bond angles.

In order to understand the contribution of CN bonds, difference spectra of $J(r)$ of samples containing different nitrogen concentrations are plotted in Fig. 2(d). Positive and negative intensities of the difference curves at a particular r are the indications of the formation and absence of the particular bond, respectively. All the three curves have a tendency of decrease of intensity at about 1.5 Å and also at about 2.0 Å explaining the decrease of CC sp^3 bonds with the increase of nitrogen percentage. Peaks at 1.15 Å and at 1.36 Å of the (9-0)%N curve could indicate the formation of C≡N and C═N (or C—N) bonds, respectively. Surprisingly an intense peak appears at 1.22 Å from the other two curves [(29-9)%N and (29-0)%N] suggesting a majority of N═N bonds with high nitrogen concentration. So it seems that at high nitrogen concentration not all nitrogen atoms are bound to the carbon atoms.

B. Interference function $[I(K)]$

The features observed from $I(K)$ [see Fig. 1(b)] are as follows. A prepeak between 2 and slightly above 3 Å^{-1}, a main peak at about 5.5 Å^{-1}, a double-peak feature between 7 and 12 Å^{-1}, and a broad one near 13 Å^{-1}. The prepeak shows a complex behavior with nitrogen concentration. For ta-C this prepeak appears at about 3.06 Å^{-1}, which is very similar to [100] reflection of diamond. A rough estimation of sp^3-bond fraction may be made (Jungnickel *et al.*[10]) from the position of this prepeak. The position of the peak at about 5.5 Å^{-1} moves towards higher K values with nitrogen per-

centage. We see that for ta-C or a-CN_{09} a hump in the region between 8.0 and 10.0 $Å^{-1}$ is intense, which is an indication of high percentage of sp^3 bonds, whereas the right side between 8.0 and 10.0 $Å^{-1}$ increases in a-CN_{29} explaining graphitization of the samples. The relative intensity of the left to the right part of this double peaks between 7 and 12 $Å^{-1}$ was found to be increased with the sp^3 fraction,[10] in agreement with our results from nitrogenated carbon films. Also compared to nitrogenated carbon the peak at $\sim$ 13.0 $Å^{-1}$ is shifted to a low-K value indicating high-sp^3 content. The peak positions of the present samples in Fig. 1(b) are compared with the peaks observed from crystalline graphite and diamond. In the nitrogen-free samples the peak at 5.48 $Å^{-1}$ corresponds to the reflection from [220] planes of diamond. This peak is sharp in ta-C, which is a good indication of tetrahedral structure of carbon. For the same sample a shoulder at 1.6 $Å^{-1}$ suggests that still some amount of sp^2 bonds are present.[10,11]

For a-CN_{09} a peak is seen at 3.06 $Å^{-1}$ as found for ta-C but the peak at 5.62 $Å^{-1}$ clearly identifies the reflection from [110] planes of graphite. So for a small percentage of nitrogen the carbon films show a mixed structure between diamond and graphite. These features suggest that the nitrogenated carbon films have a structure near to sputtered carbon. Also in a-CN_{09} the peak at 10.8 $Å^{-1}$ shows a signature of sputtered carbon.[11]

In the a-CN_{29}, the first peak at 1.92 $Å^{-1}$ arises from sp^2-rich domains and [002] reflections of graphitic regions. Also the peak around 2.9 $Å^{-1}$ is close to the reflections from [100] planes of graphite, which are commonly observed in sputtered and in glassy carbon. The most intense peak appears at 5.71 $Å^{-1}$ suggesting either the absence of [110] reflection or its coverage under the peak at 5.90 $Å^{-1}$, which rises from the graphite [200] plane.

C. Analysis of structure by electron diffraction

Observed from electron diffraction and imaging the overall structure of all the films is amorphous. In addition to the amorphous regions nanocrystalline structure can also be seen from these samples [see Figs. 3(a)–(c), inset]. So we cannot consider the structure of our films as a random mixture of only trigonal and tetrahedral bonds.

From the literature we see that the presence of sp^2 bonds or microcrystalline graphite and the sp^3 network are expected to be complementary to hold the amorphous structure.[5] However, no such microcrystalline graphitic structure but some resemblance of lattice fringes were seen.[5,11–15] The fringes arise from local sp^2-bonded clusters. Similarly, ordered graphitic planes should be found in ta-C, which give rise to a strong π^* peak in the C K-edge spectrum.[13] It was shown that sp^2-bonded carbon forms clusters within an sp^3 network in the form of sheets which minimize the elastic strain energy developed mostly by biaxial compressive stress.[14,15] From molecular dynamics calculation it has been suggested that in ta-C that sp^2-bonded atoms prefer to be arranged in pairs.[10] Also from theoretical models it is understood that more than 20% sp^3-C bonds are present in ta-C films.[11,15]

In the present study from electron microscopy we have clearly seen that nanocrystalline graphite can be found in ta-C. Figure 3(a) shows ordered lines in the TEM image of ta-C corresponding to the graphite planes. A few clear and sharp diffraction rings [Fig. 3(a), inset] from this area are identified as reflection from [002], [100], and [110] planes of graphite explaining that some parts of the film are made of ordered graphite, although the average bond length of atoms is near to diamond. We believe the presence of these sp^2-bonded network disables ta-C films to be suitable for doping even though they exhibit a large optical gap of about 2 eV.

It is surprising that nitrogenated carbon films do not show any evidence of ordered graphitic layer [Figs. 3(b) and 3(c), inset]. In the nitrogenated carbon showed several small crystalline regions with sharp diffraction rings. The experimentally observed d values and a comparative study with the theoretically predicted values are listed in Table III. The diffraction patterns [Figs. 3(b) and 3(c), inset] very often match with that of α and β phase of C_3N_4.[7,8] But like the previous reports we do not find all values of d spacing as predicted theoretically. Even some new diffraction rings could indicate a new phase of CN bonded network.

D. Analysis of structure by EELS

Carbon films prepared in a filtered cathodic arc have relatively low fraction of sp^2 bonds and high density. In the present study nitrogen gas is ionized in the arc deposition chamber either by electrons in Kaufman source or by intense carbon-ion plasma or which opens a possibility of having a high fraction of nitrogen in the films and also some local structures in the amorphous matrix. A detailed study on EELS spectra recorded from nanocrystalline regions shows a difference in position, shape, and intensity of different peaks with respect to that of amorphous regions (Bhattacharyya *et al.*[16]). Here, we concentrate on the amorphous regions of the films.

A drastic change in the position of $\pi \rightarrow \pi^*$ peak and $\pi + \sigma$ plasmon peak, as well as C K and N K edges of the samples is observed as a function of nitrogen content [see Figs. 4(a)–(c)]. In the low-energy loss region the peak corresponding to the $\pi + \sigma$ plasmon oscillation shows a shift of maximum towards lower values with the increase of nitrogen concentration [Fig. 4(a)]. The area and shape of the π^* and σ^* peaks both for C K and N K edges vary with nitrogen concentration [Figs. 4(b) and 4(c)]. Even in the nitrogen-free samples a small π^* shoulder is observed due to the presence of C sp^2 bonds. This peak becomes intense with nitrogen concentration compared to the respective σ^* peak again both for C K and N K edges. The N K edge shows an overall improvement of intensity but not continuously in the ratio of π^* and σ^* peaks. For a low nitrogen concentration it is very difficult to compare the C K edge with N K edge. Also to understand N K edge in EELS is difficult for poor resolution from the samples containing a small amount of nitrogen. Still we can see a significant difference in their line shapes, which implies that the concentration of CN single and double bond is different in local structure.[16] X-ray absorption spectra can give a detailed structure of the conduction band. It is helpful to compare our work with the N K-edge structure observed from x-ray appearance near-edge structure (XANES).[16] From XANES we see that peak at $\sim$399 eV corresponds to

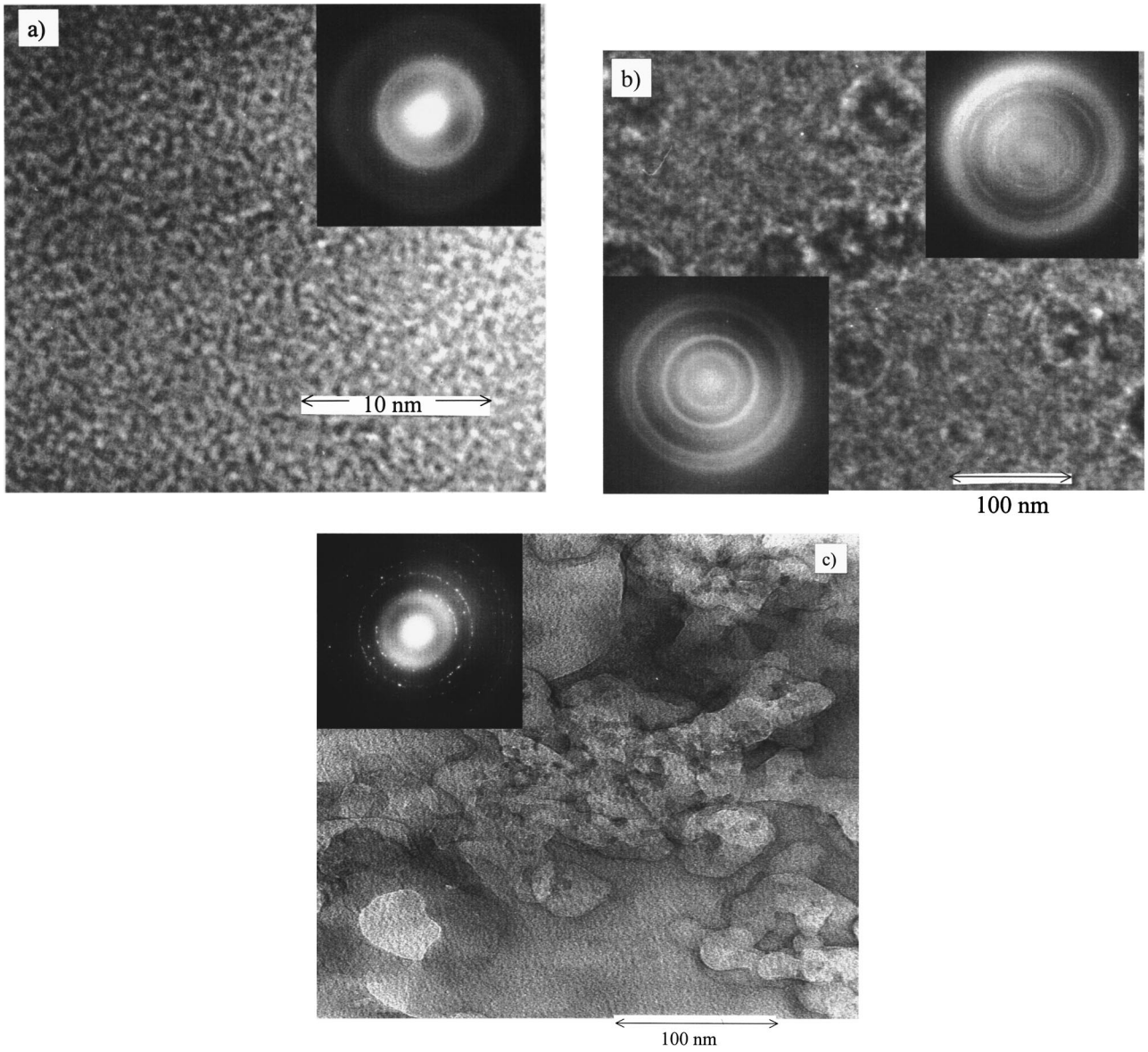

FIG. 3. TEM image collected from selected regions of carbon films having (a) 0%, (b) 19%, and (c) 29% nitrogen, respectively. Inset: Electron diffraction from the selected area shows crystalline features.

$1s \rightarrow \pi^*$ transition. This is also observed in acridine, a pyridine analogue.[16] Carbazole, a pyrrole analogue, also has a strong resonance at ~403 eV, which is assigned to a $1s \rightarrow \pi^*$. The σ^* resonance is observed at ~408 eV for amine compounds. The peak at 403.5 eV arises both from pyridine and pyrrole. The broad peak at 409 eV comes from both aromatics and saturated amine. In general, the position of the both peaks suggests an aromatic (pyridinelike) or saturated amine structure in the material.[16]

In the samples with low nitrogen percentage the π^* peaks are relatively small and they are not so prominent as the σ^* bond. For example, the σ^* transition is fairly small in the samples prepared low nitrogen ion current (a-CN_{12}). This feature is even less pronounced for the samples prepared in reactive mode (a-CN_{09}). No significant N K edge is observed for the samples having a low percentage of nitrogen (in a-CN_{04}, not shown in the figures). Also the width of σ^* peak is significantly decreased in the samples with different nitrogen concentration. For 29% nitrogen the σ^* peak is sharp relative to the other samples. The N K edge is well resolved into π^* and σ^* peaks for the samples containing a large amount of nitrogen. In a-CN_{25} π^* and σ^* are of comparable intensity. The area of π^* is maximum for a-CN_{29} and it is broad. But in a-CN_{29} again σ^* becomes more intense making the σ^* to π^* ratio high, together with a slight movement towards higher energy.

The intensity ratio of σ^* to π^* peaks is calculated from the C K and N K edges. At the C K edge this ratio decreases from 3.64 in a-CN_{09} to 1.82 in a-CN_{15} to 1.64 in a-CN_{19} and to 1.48 in a-CN_{29}. From this variation we can understand that the percentage of CC sp^2 bond increases compared to the CC sp^3 bond with the increase of nitrogen concentration. A good agreement between the increase of percentage of sp^2 bonds and optical gap with increase of nitrogen concentration has been noticed. The optical gap of ta-C is about 2 eV which is reduced to 1 eV in a-CN_{09} and finally drops to a value near to 0.3 eV in a-CN_{29} suggesting a continuous increase of the percentage of C sp^2 double bond as the nitro-

TABLE III. A comparative study between the theoretically predicted and experimentally observed *d* (distance between crystal planes) values.

β-C_3N_4 prev. obs.[a]		β-C_3N_4 calculated[a]		α-C_3N_4 calculated[a]		experimentally calculated a-CN_{29}		*d* spacing a-CN_{19}	a-CN_{09}	ta-C
5.568	(100)	5.543	(100)	5.6	(100)	5.5485	(100)	2.7386	3.6091	1.545 38
3.215	(110)	3.2	(110)	3.605	(101)	2.7710	(200)	2.2593	1.9477	1.321 72
2.784	(200)	2.771	(200)	3.233	(110)	2.3999	(101)	2.1007	1.8183	1.150 15
2.25	(101)	2.202	(101)	2.8	(200)	2.1214	(210)		1.9195	0.960 16
2.104	(210)	2.095	(210)	2.407	(201)	1.9527	(111)			
1.953	(111)	1.92	(111)	2.355	(002)	1.6735	(300)			
1.856	(300)	1.847	(300)	2.171	(102)	1.5687	(310)			
1.599	(211)	1.814	(201)	2.117	(210)	1.4660	(301)			
1.544	(310)	1.6	(220)	1.931	(211)	1.3302	(221)			
1.481	(301)	1.578	(211)	1.904	(112)	1.3013	(311)			
1.345	(221)	1.537	(310)	1.867	(300)	1.2795	(320)			
1.308	(311)	1.464	(301)	1.802	(202)	1.2299	(002)			
1.277	(320)	1.331	(221)	1.735	(301)	1.2141				
1.23	(002)	1.294	(311)	1.574	(212)	1.0844	(411)			
1.133	(321)			1.553	(310)	1.0657				
1.113	(500)			1.475	(311)	0.9759	(420)			
1.089	(411)			1.333	(222)	0.9573	(312)			
1.052	(420)			1.297	(312)	0.8994	(610)			
0.962	(312)			1.261	(213)					
0.849	(610)			1.24	(321)					

[a]See Ref. 8, values in parentheses correspond to indices of crystalline planes.

gen concentration rises up. A decrease of this ratio in the N *K* edge from 1.23 in a-CN_{09} to 1.07 in a-CN_{25} in general represents that the concentration of CN trigonal bond rises up as a function of nitrogen concentration. But a slight increase of this ratio to 1.14 in a-CN_{29} suggests that the increase of the C═N bonds is not uniform at high nitrogen content.

The similarity of π^* peaks between N *K* and C *K* edge might indicate that nitrogen is substitutional in all networks ranging from tetrahedral to trigonal structure. Here, the N *K* and C *K* edges do not look similar having different nitrogen concentration [Figs. 4(b) and 4(c)]. The intensity of the π^* peak compared to the respective σ^* peak in N *K* edge is different than that in C *K* edge. For example, in a-CN_{15} and a-CN_{25} the relative intensity of π^* peak at N *K* edge is much more than that at C *K* edge. The relative increase of the π^* peak at N *K* edge suggests an increase of the number of CN double bond compared to CN single bond, which decreases a little in a-CN_{29}.

Electron energy loss at an energy *E* should be highly specific in the way the nitrogen atom is bonded.[17] When nitrogen atoms are in a substitutional site then C *K* and N *K* edges should look similar neglecting the effect of charge transfer from C to N atoms. And for a nonsubstitutional site a difference between the near edge spectra should occur. The intensity of N *K* edge relative to C *K* edge does not necessarily indicate that more nitrogen is incorporated. It could happen in other ways due to charge transfer as indicated by Wan and Egerton.[18] Besides, all nitrogen atoms cannot be expected to substitute carbon atoms from network. Consequently, the atomic fraction of nitrogen in locally ordered CN_x structure will be different from disordered structure. So in most of the cases nitrogen is not homogeneously distributed in the films and even a major fraction is not at substitutional sites. Therefore, a film containing significantly less amount of nitrogen than what should be in a long-range order, might show local crystalline regions of C_3N_4.[8] This is also verified from our EELS measurements where C *K* and N *K* edges are significantly different.

In the previous report by Gilkes *et al.*[12] it was difficult to determine the absolute energy of N *K* edge and their relative shift. Also the local structure of CN films was different from the bulk. We find π^* bands in N *K* edge even at low percentage of nitrogen although its intensity remains poor. It seems that CN double bonds are formed at low percentage of nitrogen and CN double bonds increase with the nitrogen concentration. In a-CN_{25} sample the π^* peak in C *K* edge is much different from π^* peak in N *K* edge but this effect is less pronounced in a-CN_{29}. Also the rate of formation of C═N is higher than that of C═C bonds. An extensive study using XPS spectroscopy on the similar films showed that the structure of C 1*s* and N 1*s* peak are also different.[19] With the variation of nitrogen concentration the contribution from CN single and double bonds were also found to be different.[19] N 1*s* spectra were decomposed into three different peaks, which are located at about 398 eV, 400 eV, and 402 eV and they represented the amount of CN single, triple, and double bonds, respectively.[3] An increase of the CN single bond with nitrogen concentration relative to the CN triple and double

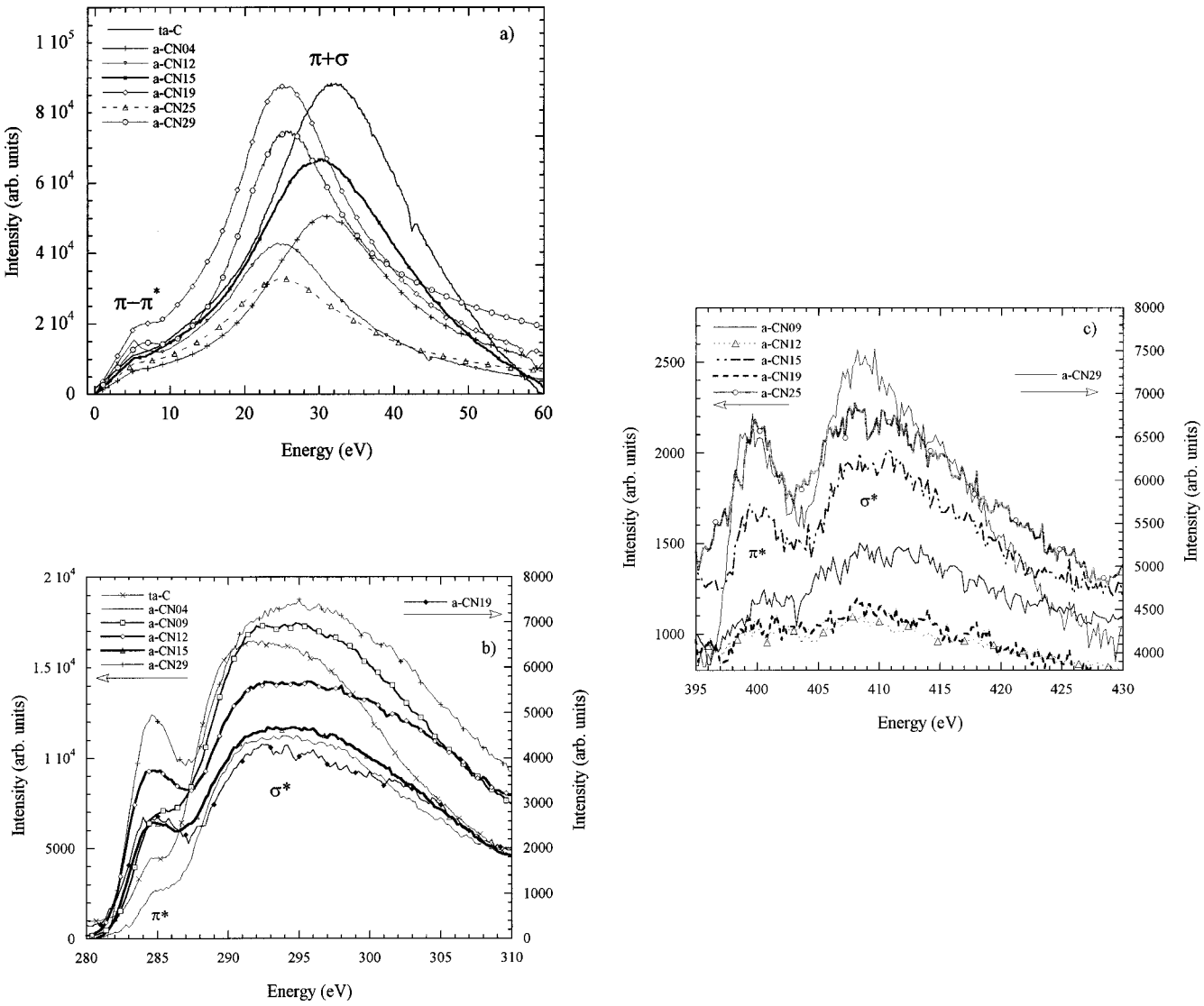

FIG. 4. EELS from different nitrogenated carbon films (a) plasmon energy loss, (b) C *K* edge, and (c) N *K* edge.

bonds was found in a-CN_{29}. A decrease of π^*/σ^* peak intensity in a-CN_{29} relative to a-CN_{25} is supported by the result from XPS analysis.[19]

Finally, the variation of CN structure can be interpreted with the help of Fig. 2(d). The difference of the $J(r)$ curves of a-CN_{29} and a-CN_{09} show the presence of molecular nitrogen establishing that the environment of N atoms is different from that of C atoms. So at high nitrogen concentration not all nitrogen atoms are bound to carbon network. At low nitrogen concentration contribution of CN triple bond is also important.

IV. CONCLUSIONS

Determination of atomic structure of ta-C as well as nitrogenated carbon films is a complicated problem. Using combined electron diffraction (RDF) and electron microscopy a thorough investigation on the structure of the films has been performed from which the following conclusions can be drawn.

(i) From RDF an increase of the amount of C═C compared to C—C bonds and also decrease of atomic number density with nitrogen concentration has been understood. (ii) This report, based on electron diffraction, clearly shows the variation of the amount of C—N, C═N, C≡N, and also N═N bonds with increase of nitrogen concentration. (iii) A clear difference between the nanocrystalline and amorphous regions of a-CN_x films has been emphasized. For instance, in ta-C films presence of ordered graphitic structure has been noticed, which might create an additional defect density of states in electronic structure of this material. From electron microscopy nanocrystalline structure of carbon-nitride, very close to β-C_3N_4, has been observed in the samples with an average atomic nitrogen concentration of 29%, which is much less than 57% as theoretically predicted. Change of microstructure of the samples with nitrogen concentration is described too. (iv) A detailed study of the N *K* edge inter-

prets the nature of CN bonds. A dissimilarity in the intensity of σ^* to π^* ratio calculated from the C K and N K edges suggests that not all nitrogen atoms are bound in substitutional sites. At high nitrogen concentration bonding between nitrogen atoms is understood from EELS as well as from the difference curves of RDF. Also the variation of the amount of C═C to C—C bonds with nitrogen concentration is found to be not connected with that of C═N to C—N bonds. In general, the amount of C═N relative to the C—N bonds increases as the nitrogen concentration rises up but it is not uniform at highest nitrogen content measured.

ACKNOWLEDGMENTS

We gratefully acknowledge C. Spaeth for measuring the nitrogen concentration in the samples. S.B. would like to thank the Alexander von Humboldt Stiftung for financial assistance.

*Author to whom correspondence should be addressed. Electronic address: somnath.bhattacharyya@physik.tu-chemnitz.de

[1] S. R. P. Silva, J. Robertson, G. A. J. Amaratunga, B. Rafferty, L. M. Brown, J. Schwan, D. F. Franceschini, and G. M. Mariotto, J. Appl. Phys. **81**, 2626 (1997).

[2] D. R. McKenzie, D. A. Muller, and B. A. Pailthorpe, Phys. Rev. Lett. **67**, 773 (1991); B. R. Djordjevic, M. F. Thorpe, and F. Wooten, Phys. Rev. B **52**, 5685 (1995).

[3] S. Bhattacharyya, C. Cardinaud, and G. Turban, J. Appl. Phys. **83**, 4491 (1998); S. Bhattacharyya, C. Vallee, C. Cardinaud, O. Chauvet, and G. Turban, *ibid.* **85**, 2162 (1999).

[4] J. Schwan, W. Dworschak, K. Jung, and H. Ehrhardt, Diamond Relat. Mater. **3**, 1034 (1994); J. Robertson and C. A. Davis, *ibid.* **4**, 441 (1995).

[5] K. W. R. Gilkes, P. H. Gaskell, and J. Yuan, Diamond Relat. Mater. **3**, 369 (1994); P. H. Gaskell, A. Sayeed, P. C. Chieux, and D. R. McKenzie, Phys. Rev. Lett. **67**, 773 (1991); J. Robertson, Surf. Coat. Technol. **50**, 185 (1992); D. R. McKenzie, D. C. Green, P. D. Swift, D. J. H. Cockane, P. J. Martin, R. P. Netterfield, and W. G. Sainty, Thin Solid Films **193/194**, 418 (1990).

[6] P. Sitch, G. Jungnickel, M. Kaukonen, D. Porezag, Th. Fraunheim, M. R. Pederson, and K. A. Jackson, J. Appl. Phys. **83**, 4642 (1998); Th. Frauenheim, G. Jungnickel, P. Sitch, M. Kaukonen, F. Weich, J. Widany, and D. Porezag, Diamond Relat. Mater. **7**, 348 (1998).

[7] D. Goldberg, Y. Bando, K. Kurashima, and T. Sasaki, Appl. Phys. Lett. **72**, 2108 (1998); J. Martin-Gil, F. J. Martin-Gil, M. Sarikaya, M. Qian, M. Jose-Yacaman, and A. Rubio, J. Appl. Phys. **81**, 2555 (1997).

[8] A. Y. Liu and M. Cohen, Phys. Rev. B **41**, 10 727 (1990); D. Li, X. Chu, S. C. Cheng, X. W. Lin, V. P. Dravid, and Y. W. Chung, Appl. Phys. Lett. **67**, 203 (1995); J. Wang, J. Lei, and R. Wang, Phys. Rev. B **58**, 11 890 (1998).

[9] S. Fahy, S. G. Louie, and M. L. Cohen, Phys. Rev. B **34**, 1191 (1986); G. Jungnickel, M. Kühn, S. Deutschmann, F. Richter, U. Stephan, P. Blaudeck, and Th. Frauenheim, Diamond Relat. Mater. **3**, 1056 (1994); B. O'Malley, I. Snook, and D. McCulloch, Phys. Rev. B **57**, 14 148 (1997); C. Z. Wang and K. M. Ho, *ibid.* **50**, 12 429 (1994).

[10] G. Galli, R. M. Martin, R. Car, and M. Parrinello, Phys. Rev. Lett. **62**, 555 (1989); F. Li and J. S. Lannin, *ibid.* **65**, 1905 (1990).

[11] S. D. Berger, D. R. McKenzie, and P. J. Martin, Philos. Mag. Lett. **57**, 285 (1988); A. R. Merchant, D. G. McCulloch, D. R. McKenzie, Y. Yin, L. Hall, and E. G. Gerstner, J. Appl. Phys. **79**, 6914 (1996); C. A. Davis, D. R. McKenzie, L. E. Hall, E. Kravtchinskaia, V. Keast, G. A. J. Amaratunga, and V. S. Veerasamy, J. Non-Cryst. Solids **170**, 46 (1994); P. H. Gaskell, A. Sayeed, P. C. Chieux, and D. R. McKenzie, Philos Mag. B **66**, 155 (1992).

[12] K. W. R. Gilkes, P. H. Gaskell, and J. Yuan, J. Non-Cryst. Solids **164-166**, 1107 (1993).

[13] S. R. P. Silva, S. Xu, B. K. Tay, H. S. Tan, H.-J. Scheibe, M. Chhowalla, and W. I. Milne, Thin Solid Films **290-291**, 317 (1996).

[14] E. G. Gerstner, P. B. Lukins, D. R. McKenzie, and D. G. McCulloch, Phys. Rev. B **54**, 14 504 (1996).

[15] K. W. R. Gilkes, P. H. Gaskell, and J. Robertson, Phys. Rev. B **51**, 12 303 (1995).

[16] S. M. Kirtley, O. C. Mullins, J. V. Elp, and S. P. Cramer, Fuel **72**, 133 (1993); S. Bhattacharyya, M. Hietschold, and F. Richter, Diamond Relat. Mater. (to be published).

[17] C. A. Davis, D. R. McKenzie, L. E. Hall, E. Kravtchinskaia, V. Keast, G. A. J. Amaratunga, and V. S. Veerasamy, Philos. Mag. B **69**, 1133 (1994).

[18] L. Wan and R. F. Egerton, Thin Solid Films **279**, 34 (1994).

[19] C. Spaeth, M. Kühn, U. Kreissig, and F. Richter, Diamond Relat. Mater. **6**, 626 (1997).